Hetero- and homoepitaxial Nd3+-doped LaF3 thin films grown by molecular beam epitaxy: A spectroscopic study

F. Lahoz, E. Daran, X. Zhang, A. Muñoz-Yagüe, R. Cases et al.

Related Articles

Controlling spatial distribution of thermal poling induced second-order optical nonlinearity with multilayered structures
Appl. Phys. Lett. 101, 101101 (2012)

Optical characteristic of sol-gel synthesized lead lanthanum titanate-cobalt iron oxide multiferroic composite thin film
J. Appl. Phys. 112, 043520 (2012)

Electrical and Fourier transform infrared properties of epitaxial SmNiO3 tensile strained thin film
Appl. Phys. Lett. 101, 091908 (2012)

Ellipsometrically determined optical properties of nickel-containing tungsten oxide thin films: Nanostructure inferred from effective medium theory
J. Appl. Phys. 112, 044308 (2012)

Ge2Sb2Te5 phase-change films on polyimide substrates by pulsed laser deposition
Appl. Phys. Lett. 101, 031905 (2012)

Additional information on J. Appl. Phys.

Journal Homepage: http://jap.aip.org/

Journal Information: http://jap.aip.org/about/about_the_journal

Top downloads: http://jap.aip.org/features/most_downloaded

Information for Authors: http://jap.aip.org/authors

Hetero- and homoepitaxial Nd^{3+}-doped LaF_3 thin films grown by molecular beam epitaxy: A spectroscopic study

F. Lahoz,[a] E. Daran, X. Zhang,[b] and A. Muñoz-Yagüe
LAAS–CNRS, 7 avenue du Colonel Roche, 31077 Toulouse, France

R. Cases and R. Alcalá
ICMA, Universidad de Zaragoza–CSIC, 50009 Zaragoza, Spain

Hetero- and homoepitaxial Nd^{3+}-doped LaF_3 thin films have been grown by molecular beam epitaxy. Two different orientations of CaF_2 substrates, (111) and (110), have been used for the heteroepitaxial structures. High-resolution emission and excitation spectra as well as the decay time of the emission have been measured. The spectroscopic measurements demonstrate that one Nd^{3+} site is present in the LaF_3 layers grown on CaF_2(111) substrates but two slightly different Nd^{3+} centers are resolved in the films on CaF_2(110) substrates. One Nd^{3+} site has been found in the homoepitaxial sample. Slight differences are observed between the centers found in the LaF_3 layers and the one observed in the Nd^{3+}-doped LaF_3 bulk crystal. For the homoepitaxial layer, the linewidths are similar to those of the bulk crystals, whereas for the heteroepitaxial layers, a broadening is observed. © *1999 American Institute of Physics.* [S0021-8979(99)00519-8]

I. INTRODUCTION

Rare-earth (RE) -doped thin films are of increasing interest because of their application as active waveguides in optoelectronic devices. Miniature solid-state lasers and amplifiers activated with RE ions could be associated with semiconductor lasers in this type of application. Compact and efficient optical systems could thus be obtained using thin-film waveguides, and the light confinement achieved in planar and channel waveguides would also reduce the laser pumping threshold and increase the gain per unit pump power as compared to bulk materials.[1–3] For certain specific applications, fluoride materials have been shown to be more suitable laser host matrices than oxides, owing to their lower phonon frequencies, which reduce the nonradiative relaxation processes of the excited RE ions increasing the lifetime of the emitting levels.[4]

Molecular beam epitaxy (MBE) is an ultra-high-vacuum thin-film growth technique, conventionally employed for semiconductor devices. MBE has also demonstrated its suitability to fabricate active fluoride waveguide structures on dielectric[5] or semiconductor[1] substrates, and to incorporate high-RE concentrations without quenching of the luminescence and keeping an excellent crystallinity of the layer.[5]

CaF_2:Nd^{3+} thin films grown by MBE on CaF_2 substrates have been extensively studied.[6–8] Trivalent Nd^{3+} ions enter in divalent Ca^{2+} sites. A charge compensation mechanism is needed to ensure the global electrical neutrality of the crystal. This is provided by interstitial fluoride ions. Depending on the different relative positions of the interstitial F^- with respect to the Nd^{3+} ion, different configurations are possible.

For high enough dopant concentrations the RE ions and their associated F^- interstitials aggregate to form complex centers. In particular, clusters of two and four Nd^{3+}–F^- pairs have been identified in CaF_2:Nd/CaF_2 layers.[8]

For some applications it is desirable to avoid the broadening of the emission lines associated with the presence of different configurations of the RE ions in the crystal and to have just one type of impurity center with narrow luminescence lines which increase the effective absorption and emission cross sections at specific wavelengths. In order to avoid the influence of interstitial F^- ions, Nd^{3+}-doped LaF_3 thin films have been grown. LaF_3 has a trivalent cation and no charge compensation mechanism is needed when the Nd^{3+} ions are incorporated as a dopant. Nd^{3+} ions enter in La^{3+} sites and only one center is expected.

Previous work on LaF_3:Nd^{3+} thin films on CaF_2 substrates has shown encouraging results. The refractive index difference between the layer and the substrate allows both the pumping and the emitted light to be guided into the film. Laser emission at 1060 nm was obtained at room temperature (RT).[9] However, no laser emission was found in CaF_2:Nd/CaF_2 layers. This reveals the great interest in using LaF_3 as a matrix for trivalent RE ions. To acquire a deeper knowledge of these systems in order to optimize them, a photoluminescence study of these materials has been carried out.

In this article a comparative spectroscopic study oriented towards laser applications of Nd^{3+}-doped hetero- and homoepitaxial LaF_3 layers grown by MBE on CaF_2 and LaF_3 substrates is presented. Two different orientations of the CaF_2 substrates, (111) and (110), have been considered for the heteroepitaxial structures. The CaF_2(111) surface shows a hexagonal geometrical arrangement of the ions which could be, in principle, the most suitable for the growth of the hexagonal tysonite structure of LaF_3. On the other hand, the

---

[a] Permanent address: ICMA, Universidad de Zaragoza–CSIC, Pza. San Francisco s/n, 50009 Zaragoza, Spain. Electronic mail: lahoz@laas.fr
[b] Permanent address: Laboratory of Excited State Processes, Chinese Academy of Sciences, 130021 Changchun, China.

$CaF_2(110)$ substrates show a technological advantage as (110) planes are perpendicular to the (111) cleavage planes. In this case, the end faces of the waveguiding systems can be obtained by cleavage rather than by a long and arduous cutting and polishing process. High-resolution emission and excitation spectroscopy as well as lifetime measurements have been performed. As expected, only one Nd^{3+} center has been found in $LaF_3:Nd^{3+}/CaF_2(111)$ samples. However, two slightly different centers have been resolved in $LaF_3:Nd^{3+}/CaF_2(110)$ layers. The influence of the substrate orientation on the spectroscopic properties of Nd^{3+} ions is discussed.

The Nd^{3+}-doped LaF_3 homoepitaxial layer shows a narrowing of the emission lines by a factor of about 3 as compared with the heteroepitaxial ones, which are inhomogeneously broadened. This reduction of the linewidth is considered as an improvement in the crystal quality of the layers in order to increase the laser performance. All the results are compared with those of Nd^{3+}-doped LaF_3 bulk crystals.

II. EXPERIMENT

The monocrystalline thin films studied in this article were grown under ultra-high-vacuum conditions by MBE using separate effusion cells for LaF_3 and NdF_3. CaF_2 substrates with (111) and (110) orientation and LaF_3 substrates were degreased and mounted on molybdenum blocks. For all the layers, the evaporation rate of the LaF_3 effusion cell was kept constant, corresponding to a growth rate of 0.6 μm/h, while the NdF_3 cell temperature was varied from 988 to 1073 °C in order to obtain Nd concentrations ranging from 0.5 to 5 mol %. Previously, the LaF_3 and NdF_3 effusion cells were calibrated separately by measuring the deposited layer thickness as a function of the cell temperature. The layers under study were grown at a substrate temperature of about 550 °C. The thickness of the layers was measured by profilometry and ranged from 0.7 to 4 μm.

Luminescence spectra were obtained by two methods. First, under excitation with the 514.5 nm line of an Ar^+ laser using a $f = 1$ m monochromator and a cooled Ge photodiode for the detection. Second, high-resolution measurements were performed with the following setup. A pulsed 1.064 μm Nd:YAG laser was frequency doubled to pump a tunable dye laser, the output of which was passed through a H_2 Raman cell and its first Stokes was used to excite the samples in the 860–870 nm region. The luminescence was focused on a $f = 1.7$ m monochromator and detected by a silicon photodiode. The reproducibility of these measurements has been estimated to be better than 0.1 nm.

III. RESULTS AND DISCUSSION

A. Heteroepitaxial layers

Figure 1 shows two regions of the emission spectrum of a $LaF_3:1$ mol % Nd layer grown on a $CaF_2(111)$ substrate under excitation at 514.5 nm and measured at 25 K. The 850–910 nm region corresponds to the $^4F_{3/2} \rightarrow {}^4I_{9/2}$ transition [Fig. 1(a)] and the 1035–1075 nm region to the $^4F_{3/2}$
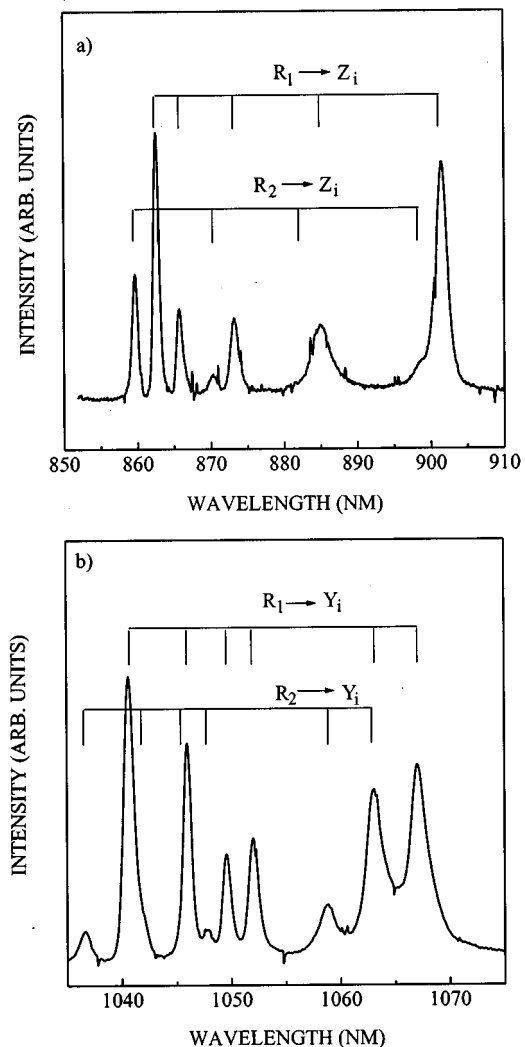

FIG. 1. Photoluminescence spectra of a $LaF_3:1$ mol %Nd/$CaF_2(111)$ layer excited at 514.5 nm at 25 K. The bar diagrams correspond to the transitions between the Stark levels of the $^4F_{3/2}$ multiplet and the (a) $^4I_{9/2}$ and (b) $^4I_{11/2}$ manifolds.

$\rightarrow {}^4I_{11/2}$ transition [Fig. 1(b)]. Due in part to the focusing of the excitation laser, the sample is heated and thus the two Stark levels of the $^4F_{3/2}$ excited level (labeled R_1 and R_2) are thermally populated. The bar diagrams correspond to the transitions from the R_1 and R_2 levels of the $^4F_{3/2}$ manifold to the $^4I_{9/2}$ [Fig. 1(a)] and $^4I_{11/2}$ [Fig. 1(b)] multiplets (labeled Z_i and Y_i, respectively).

From each of the R_1 and R_2 excited levels, five emission lines are detected to the Stark sublevels of the $^4I_{9/2}$ ground state and six to those of the $^4I_{11/2}$ manifold. It seems that only one Nd^{3+} center is present in $LaF_3:1\%Nd/CaF_2(111)$ thin films, as expected. Similar spectra have been observed for 0.5, 2.5, and 5 at. % Nd concentrations. All these layers have a thickness of about 3.6 μm. The highest luminescence intensity appears for a Nd nominal concentration of 1 mol %. At higher dopant contents quenching of the luminescence occurs.

The same luminescence measurements have been performed on Nd-doped LaF_3 layers grown at the same time on $CaF_2(110)$ substrates. The Nd concentrations and the layer
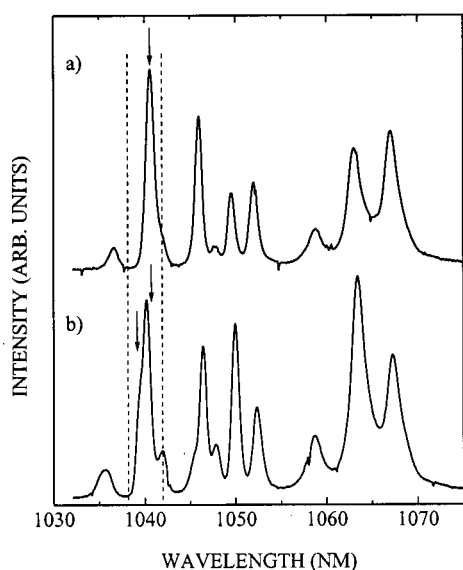
FIG. 2. Emission spectra of Nd^{3+} in the $^4F_{3/2} \rightarrow {}^4I_{11/2}$ region excited at 514.5 nm for LaF_3 layers grown on two different CaF_2 substrate orientations: (a) (111) and (b) (110). The dotted lines enclose the region where a broadening can be appreciated. Arrows indicate the wavelength used for site selective spectroscopy.

FIG. 3. Excitation spectra of the $^4I_{9/2} \rightarrow {}^4F_{3/2}$ Nd^{3+} transition measured at 10 K for: (a) LaF_3:1 mol %Nd/CaF_2(111) detected at 1040.7 nm; (b) LaF_3:1 mol %Nd/CaF_2(110) detected at 1040.3 nm; (c) LaF_3:1 mol %Nd/CaF_2(110) detected at 1039.5 nm; (d) LaF_3: 2 mol % bulk crystal detected at 1040.5 nm; and (e) LaF_3:1 mol %Nd/LaF_3 detected at 1040.7 nm.

thickness were the same as on the CaF_2(111) substrates. The maximum of the luminescence intensity is also obtained for the 1 mol % Nd-doped sample. When exciting at 514.5 nm, the emission spectrum in the 850–910 nm and in the 1035–1075 nm regions show the same pattern as that in Fig. 1. However, a broadening of some of the lines is observed. Figure 2 shows the emission spectrum corresponding to the $^4F_{3/2} \rightarrow {}^4I_{11/2}$ transition under excitation at 514.5 nm for a LaF_3:1 mol %Nd/CaF_2(110) layer. The spectrum of the same layer on a CaF_2(111) substrate is also reproduced for comparison. The number of lines in both spectra is the same, however, the line at about 1040 nm (between the dashed markers in Fig. 2) is broader in the spectrum associated with the CaF_2(110) substrate and a shoulder is observed on its high-energy side. The line corresponds to the transition from the R_1 to the Y_1 Stark levels of the $^4F_{3/2}$ and $^4I_{11/2}$ multiplets, respectively. The shoulder is observed for all the Nd concentrations studied in the layers grown on the CaF_2(110) substrate.

In order to obtain more information, high-resolution excitation and emission measurements have been performed. Figures 3(a)–3(c) show the excitation spectra recorded at 10 K in the 860–868 nm region, which corresponds to the transition from the $^4I_{9/2}$ ground state to the $^4F_{3/2}$ excited state. The arrows in Fig. 2 indicate the detection wavelengths used. For the LaF_3:1 mol %Nd/CaF_2(111) layer the detection wavelength was set at 1040.7 nm, which corresponds to the maximum of the emission line. Two lines appear in the excitation spectrum corresponding to the transition from the Z_1 Stark level of the $^4I_{9/2}$ manifold to the R_1 and R_2 Stark levels of the $^4F_{3/2}$ multiplet [Fig. 3(a)]. This spectrum together with those of Fig. 1 agrees with the assumption of only one Nd^{3+} center in the film.

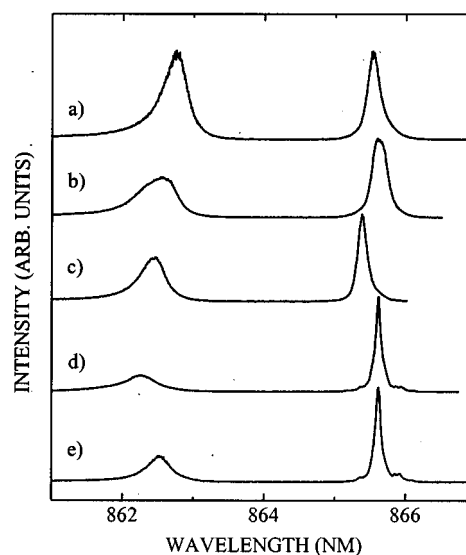On the other hand, in the LaF_3:1 mol %Nd/CaF_2(110) sample the detection wavelengths were set at the sides of the emission line indicated by the arrows in Fig. 2, trying to resolve the possible contributions of different centers to the emission spectrum. Indeed, two different excitation spectra were observed detecting at 1040.3 and at 1039.5 nm [Figs. 3(b) and 3(c), respectively]. This result indicates the presence of two different Nd^{3+} centers (labeled center 1 and center 2) in the LaF_3 layers grown on a CaF_2 substrate oriented in the (110) direction, in contrast with the films grown on a (111)-oriented CaF_2 substrate, which have just one Nd^{3+} site. From these spectra the splitting of the R_1 and R_2 Stark levels of the $^4F_{3/2}$ manifold can be calculated. For center 1 and center 2 in the layer grown on a CaF_2(110) substrate this gives $\Delta E = 41.5\,\mathrm{cm}^{-1}$ and $\Delta E = 40.2\,\mathrm{cm}^{-1}$, respectively, and for the Nd^{3+} center in the film on a CaF_2(111) substrate $\Delta E = 37.2\,\mathrm{cm}^{-1}$. These small differences in the energy splitting are due to slight variations in the local surrounding of the Nd^{3+} ions, which produce a different crystal field.

Taking advantage of the different excitation spectra of the two centers in Figs. 3(b) and 3(c), site selective excitation has been performed to obtain the emission spectra associated with each of them. The luminescence of the LaF_3:1 mol %Nd/CaF_2(111) layer was also detected, with excitation at 865.5 nm. The emission spectra associated with the $^4F_{3/2} \rightarrow {}^4I_{11/2}$ transition are shown in Figs. 4(a)–4(c). The sample temperature was about 10 K. At this temperature the R_2 Stark level of the $^4F_{3/2}$ state is not thermally populated and the only populated level is the R_1 Stark level, from which luminescence occurs. The spectrum of LaF_3:1 mol %Nd/CaF_2(111) is presented in Fig. 4(a). Six lines are observed which are associated with the six Stark

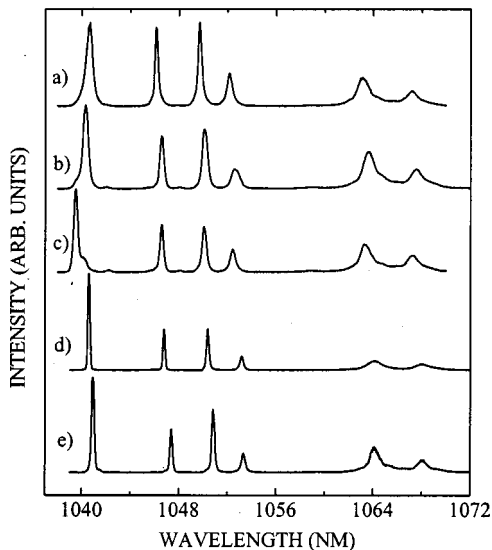FIG. 4. Emission spectra of the $^4F_{3/2} \rightarrow ^4I_{11/2}$ Nd^{3+} transition measured at 10 K for: (a) LaF_3:1 mol %Nd/CaF_2(111) excited at 865.5 nm; (b) LaF_3:1 mol %Nd/CaF_2(110) excited at 865.6 nm; (c) LaF_3:1 mol %Nd/CaF_2(110) excited at 865.4 nm; (d) LaF_3:2 mol % bulk crystal excited at 865.6 nm; and (e) LaF_3:1 mol %Nd/LaF_3 excited at 865.6 nm.

levels of the $^4I_{11/2}$ manifold. This spectrum is in agreement with the existence of only one Nd^{3+} center in this layer. Figures 4(b) and 4(c) show the emission spectra of LaF_3:1 mol %Nd/CaF_2(110) exciting at 865.6 and at 865.4 nm, respectively. In both cases, a pattern of six lines is obtained but the positions of the lines are slightly different. This is clearly seen in the line at about 1040 nm. The broad line which appears in Fig. 2(b) can be understood now as the envelope of the lines at 1039.5 and 1040.3 nm observed in Figs. 4(b) and 4(c), respectively. It can be concluded from the emission and excitation spectra that two different centers in the LaF_3:1 mol %Nd/CaF_2(110) layer have been resolved.

This is quite an unexpected result as only one Nd^{3+} center has been observed in Nd^{3+}-doped LaF_3 bulk crystals.[10] Nd^{3+} ions enter in a La^{3+} position and just one site is expected. However, for the MBE-grown thin layers the crystal orientation of the CaF_2 substrate seems to play a role.

To check if one of the two Nd^{3+} centers in LaF_3 on the CaF_2(110) substrates could be related to strained regions of the layer close to the interface, a new LaF_3:1 mol %Nd/CaF_2(110) film was grown under the same experimental conditions, but with a thickness of about 0.7 μm, i.e., five times thinner than the layer studied in Figs. 4(b)–4(c). If one of the centers were associated with the interface, the ratio of the intensities of the emission lines of center 1 and center 2 would change from the 0.7-μm-thick sample to the 3.6-μm-thick sample. However, no significant change in the ratio between the intensities of centers 1 and 2 was detected in the 0.7 μm film as compared with the 3.6 μm one. These results indicate that the two different Nd^{3+} sites in the LaF_3 layers grown on (110)-oriented CaF_2 substrates are present throughout the layer and neither of them is preferentially placed at the substrate–layer interface.

From Figs. 3(a)–3(c) and 4(a)–4(c) it can be observed that neither of the spectra of the two centers which appear on a (110)-oriented substrate coincide with that of the center on a (111)-oriented CaF_2 substrate. It could be interesting to know if any of them corresponds to the one observed in Nd^{3+}-doped LaF_3 bulk crystals. Figures 3(d) and 4(d) show the excitation and emission spectra of a 2 mol % Nd^{3+}-doped LaF_3 bulk crystal measured at 10 K. The line positions do not coincide with either of those of the two centers in LaF_3:1 mol %Nd/CaF_2(110) or with those of the Nd^{3+} site in LaF_3:1 mol %Nd/CaF_2(111). The splitting of the Stark levels of the $^4F_{3/2}$ multiplet deduced from Fig. 3(d) is $\Delta E = 44$ cm^{-1}, which is bigger than that found in the films. Another significant difference is the narrowing of the lines in the bulk sample as compared with the heteroepitaxial layers. The linewidth of the emission line at about 1040 nm in the bulk crystal is 0.2 nm and for the films grown on CaF_2 it is about 0.6 nm. A broadening of the lines by about a factor of 3 is observed in the heteroepitaxial films due to an inhomogeneous distribution of those centers. To date, we do not have an explanation for the presence of the two Nd^{3+} centers in the films grown on CaF_2(110) substrates. X-ray diffraction measurements would be useful to better understand this problem.

It is well known for heteroepitaxial structures that the mismatch of the lattice parameters and the difference in the thermal expansion coefficients between the substrate and the layer can induce some residual stress which should produce some crystalline defects, reducing the homogeneity of the sample and broadening the emission lines of the Nd^{3+} ions.[11] It could also be possible that an inhomogeneous distribution of centers could be intrinsically associated with the MBE growth process, for which the thermodynamic conditions differ greatly from those of bulk crystal growth. In order to answer this question and to optimize the crystal quality of the layers, a Nd^{3+}-doped LaF_3 homoepitaxial layer has been studied.

B. Homoepitaxial layers

The strains due to the lattice mismatch and thermal coefficient differences between the layer and the substrate can be avoided in a homoepitaxial growth, i.e., depositing a Nd-doped LaF_3 layer on a LaF_3 substrate.

Figures 3(e) and 4(e) show the excitation and emission spectra of a LaF_3:1 mol %Nd/LaF_3 layer of about 4 μm thickness measured at 10 K. The number of lines indicates that just one Nd^{3+} site exists in this sample. Their positions are slightly different from those of the bulk crystal, as well as the splitting of the Stark levels of the $^4F_{3/2}$ multiplet deduced from Fig. 3(e), $\Delta E = 41.5$ cm^{-1}. However, the linewidths are very similar.

The widths of the emission and excitation lines indicate that the inhomogeneous broadening detected in the heteroepitaxial layers is likely to be due to the strain, disorder, and/or defects originated by the lattice mismatch and thermal expansion differences between the layer and the substrate and that this is avoided in homoepitaxial MBE-grown films. These results also suggest that the crystal quality obtained in
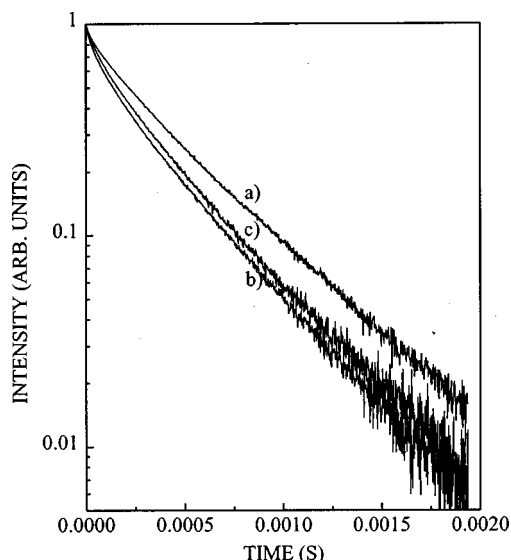
FIG. 5. Luminescence decay in center 1 in LaF$_3$:1 mol %Nd/CaF$_2$(110) at (a) 10 K, (b) 30 K, and (c) 100 K.

FIG. 6. Lifetime of the $^4F_{3/2}$ level of Nd^{3+} as a function of temperature in LaF$_3$:1 mol %Nd/CaF$_2$(111), center 1 and center 2 in LaF$_3$:1 mol %Nd/CaF$_2$(110) and LaF$_3$:1 mol %Nd/LaF$_3$ layers. Dotted lines are only guides to the eye.

the homoepitaxial growth is similar to that of the bulk crystal. It is important to remark that a good crystal quality ensures low propagation losses, which is a main parameter to optimize materials for laser applications. To obtain waveguiding in these homoepitaxial films, doping with another additional impurity, such as CeF$_3$,[12] can increase the refractive index of the layer. A complete study and characterization of this homoepitaxial system for laser applications will be shortly carried out to reduce the laser pumping threshold and to increase the slope efficiency found in LaF$_3$:1 mol %Nd/CaF$_2$(111) heteroepitaxial layers.[9]

C. Decay time measurements

Another important parameter to characterize the emitting levels of RE ions for laser applications is the decay time.

The decay of the luminescence of the $^4F_{3/2}$ level of Nd^{3+} has been measured in all the layers. In the LaF$_3$:1 mol %Nd/CaF$_2$(110) sample, centers 1 and 2 were selectively excited to obtain the decay curve of each of them. As an example, the decay of center 1 measured at different temperatures is shown in Fig. 5. A nonexponential curve is clearly observed. The decay is faster at the beginning and slower after some hundreds of microseconds. Even at this relatively low Nd^{3+} concentration (1 mol %), cross relaxation is already occurring and gives rise to these kinds of nonexponential decay curves, which are also observed for the other Nd^{3+} concentrations.

In order to compare the different decay curves a criterion has been established to associate a decay time τ with each decay curve. Since the decay at long times seems to be exponential, the first 500 μs have been neglected and the rest of the curve has been fitted to an exponential function. The temperature dependence of τ has been measured in 1 mol % Nd-doped LaF$_3$/CaF$_2$(110), LaF$_3$/CaF$_2$(111), and LaF$_3$/LaF$_3$ samples. The results are shown in Fig. 6. The estimated accuracy of these values is about $\pm$ 5%. In all the measurements a nonexponential decay was observed. The thermal
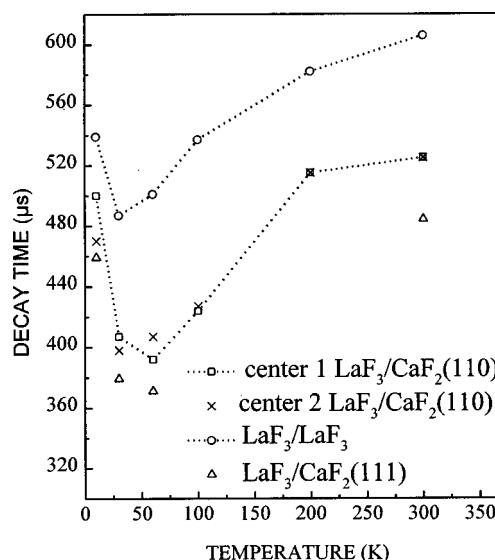
evolution of τ is similar to the one observed in Nd^{3+}-doped LaF$_3$ bulk samples, which has been explained as due to the difference between the combined probabilities of the radiative transition from the ground and excited components of the excited state $^4F_{3/2}$ and to the cross-relaxation transition probability between energy levels of Nd^{3+} ions.[13,14] The higher τ values obtained in the homoepitaxial sample could be due to small differences in the Nd^{3+} content of the samples.[14] No significant difference is detected in the lifetime of center 1 and center 2 in the LaF$_3$/CaF$_2$(110) layer at any temperature. The small differences in the local environment of center 1 and center 2 are responsible for slight shifts in the excitation and emission spectral [Figs. 3(b), 3(c), 4(b) and 4(c)] but do not give a place for any detectable change in τ.

IV. CONCLUSIONS

High-resolution excitation and emission spectroscopy and lifetime measurements have been performed on hetero- and homoepitaxial Nd^{3+}-doped LaF$_3$ layers. In the heteroepitaxial layers, the highest luminescence intensity is obtained in the samples doped with 1 mol %. One Nd^{3+} center has been found in the films grown on CaF$_2$(111) substrates. However, two slightly different centers have been resolved in the layers deposited on CaF$_2$(110) substrates. Neither of the two sites observed in the films grown on CaF$_2$(110) substrates is specifically associated with the layer–substrate interface. On the contrary, both centers seem to be present throughout the thickness of the film. None of the centers coincide with the single center found in LaF$_3$:Nd^{3+} bulk crystals. The linewidth of the emission lines of Nd^{3+} ions in the heteroepitaxial layers is about three times larger than in the bulk sample, indicating a broadening of the lines associated with an inhomogeneous distribution of the Nd^{3+} centers, which is not present in the bulk crystal.

A single site has been found in the homoepitaxial Nd^{3+}-doped LaF_3/LaF_3 sample studied. The positions of the emission and excitation lines are once again slightly different from those in Nd^{3+}-doped LaF_3 bulk crystals. Both the emission and excitation spectra as well as the lifetime measurements indicate that very small crystal-field differences exist among all the observed centers. Nevertheless, similar linewidths to those in the bulk crystal are obtained in the homoepitaxial film. The presence of strains, defects, and disorder in the heteroepitaxial layers originating from the lattice mismatch and thermal expansion differences between the layer and the substrate, causes an inhomogeneous broadening of the luminescence spectra which is avoided in the homoepitaxial sample. This suggests that a similar crystal quality to that of LaF_3 bulk crystals is reached in the homoepitaxial growth. This is important for laser applications as improvements in the crystal quality of the layer could play a significant role in the minimization of propagation losses in the waveguide and, consequently, in the optimization of the laser performance.

ACKNOWLEDGMENTS

[1] R. A. MacFarlane, M. Lui, and D. Yap, IEEE J. Sel. Top. Quantum Electron. **1**, 82 (1995).

[2] D. Pelenc, B. Chambaz, I. Chartier, B. Ferrand, C. Wyon, D. P. Shepherd, D. C. Hanna, A. C. Large, and A. C. Tropper, Opt. Commun. **115**, 491 (1995).

[3] D. P. Shepherd, C. T. A. Brown, T. J. Warburton, D. C. Hanna, A. C. Tropper, and B. Ferrand, Appl. Phys. Lett. **71**, 876 (1997).

[4] R. S. Quimbly, Mater. Sci. Forum **32-33**, 551 (1988).

[5] E. Daran, R. Legros, A. Munoz-Yagüe, C. Fontaine, and L. E. Bausa, J. Appl. Phys. **76**, 270 (1994).

[6] L. E. Bausa, R. Legros, and A. Munoz-Yagüe, Appl. Phys. Lett. **59**, 152 (1991).

[7] L. E. Bausa, R. Legros, and A. Munoz-Yagüe, J. Appl. Phys. **70**, 4485 (1991).

[8] L. E. Bausa, E. Camarillo, J. Garcia Sole, F. Jaque, R. Legros, and A. Munoz-Yagüe, Solid State Commun. **85**, 257 (1993).

[9] E. Daran, D. P. Shepherd, T. Bhutta, and C. Serrano, Electron. Lett. **35**, 398 (1999).

[10] H. H. Caspers, H. E. Rast, and R. A. Buchanan, J. Chem. Phys. **42**, 3214 (1965).

[11] L. E. Bausa, C. Fontaine, E. Daran, and A. Munoz-Yagüe, J. Appl. Phys. **72**, 499 (1992).

[12] R. Laiho and M. Lakkisto, Philos. Mag. B **48**, 203 (1983).

[13] C. K. Asawa and M. Robinson, Phys. Rev. **141**, 251 (1966).

[14] Yu. K. Voron'ko, T. G. Mamedov, V. V. Osiko, A. M. Prokhorov, V. P. Sakun, and I. A. Shcherbakov, Sov. Phys. JETP **44**, 251 (1976).